

Preservation and Control of Proton Polarization Direction for Spin Experiments at the Nuclotron/JINR

E. D. Tsyplakov^{a,c,*}, Yu. N. Filatov^{a,c}, A. M. Kondratenko^{a,b}, M. A. Kondratenko^{a,b}, S. V. Vinogradov^{a,c},
A. V. Butenko^a, V. P. Ladygin^c, V. A. Lebedev^c, E. M. Syresin^c, and E. A. Butenko^c

^a *Moscow Institute of Physics and Technology (National Research University), Dolgoprudny, Moscow region, Russia*

^b *Science and Technique Laboratory Zaryad, Novosibirsk, Russia*

^c *Joint Institute for Nuclear Research, Dubna, Russia*

**e-mail: tsyplakov.ed@phystech.edu*

Received August 7, 2025; revised October 1, 2025; accepted October 1, 2025

The possibility of conducting experiments with polarized protons at the Nuclotron of the NICA accelerator complex at JINR (Dubna) is under discussion. To preserve polarization during beam acceleration a partial siberian snake is supposed to be used based on dynamic superconducting solenoids developed at JINR. Design options for a solenoid snake in the Nuclotron, both with and without compensation of betatron coupling, have been proposed. Spin orientation control for experiments with an extracted proton beam in a continuous momentum range is achieved with a spin rotator based on longitudinal and transverse magnetic fields, located in the beam transport channel to the external target. At discrete energies, occurring approximately in 0.5 GeV steps, which correspond to integer spin resonances, the polarization direction at internal and external targets can be changed without a spin rotator, applying spin navigators based on weak magnetic fields, located inside the Nuclotron.

DOI: 10.1134/S0021364025608231

INTRODUCTION

The NICA collider at the Laboratory of High Energy Physics (LHEP) of the Joint Institute for Nuclear Research (JINR, Dubna), scheduled for launch in 2025, is the largest multifunctional project in Russia in the field of nuclear physics and high-energy physics [1]. The collider is designed for the collision of counter-beams of relativistic nuclei in the Multi-Purpose Detector (MPD) [2] and counter-beams of polarized protons and deuterons in the Spin Physics Detector (SPD) [3]. The NICA collider is optimal for studying the dynamics of the transition from a quark-gluon plasma during the process of cooling the hot Universe into the observed baryonic matter. This is the first priority of NICA's work with nuclear collisions in MPD. In the second stage program with counter-beams in the SPD one of the central tasks is the solution so-called "spin crisis": quarks are the carriers of the baryon and electric charge of nucleons, but only a small part of the nucleon's spin [4, 5].

Injection of heavy ions and polarized light nuclei is carried out from the existing superconducting synchrotron Nuclotron [6]. The maximum particle momentum in the Nuclotron is limited by the characteristics of the standard superconducting dipoles and is equal to 12 GeV/c. The possibility of conducting

experiments with extracted polarized proton and deuteron beams from the Nuclotron was relevant before, it will become especially important after the collider will be put into operation. After the injection of heavy ions into the collider for experiments in the MPD the Nuclotron will be idle most of the time. The SPD detector is planned to be commissioned no earlier than 2030, so the only current opportunity for working with polarized beams within the NICA complex is experiments at the Nuclotron, which is equipped with the necessary facilities for this: the SPI polarized ion source [7] provides beams of polarized deuterons and protons for various spin modes, and polarization measurement is carried out with polarimeters at an internal target [8, 9] and on the extracted beam [10]. Currently the DSS (Deuteron Spin Structure) and ALPOM-2 experiments are being implemented on the internal and extracted beams of the Nuclotron respectively. The DSS project [11] is aimed at investigating the spin structure of the deuteron. The ALPOM-2 project is being carried out to obtain new data on the effective analyzing powers in neutron and proton interaction reactions with nuclei [12, 13]. It is proposed to conduct research on spin-dependent effects in nucleon-nucleon, nucleon-nucleus and deuteron-nucleus interaction processes at the BM@N (Baryonic Matter at Nuclotron) facility using a polarized extracted deuteron beam [14].

To conduct experiments with polarized beams extracted from the Nuclotron it is necessary to solve the problem of preserving polarization during the beam acceleration and to ensure control over the spin orientation when delivering the beam to the target.

The primary polarization loss of the beam occurs during the crossing of spin resonances [15]. The strongest of these are the intrinsic spin resonances, which are associated with the betatron oscillations of the beam. The other resonances are related to distortions of the magnetic lattice caused by manufacturing errors and misalignment of the structural elements, by non-linear effects of spin and orbital motion, and by the inclusion of corrective and functional elements (dipoles, quadrupoles, sextupoles, etc.). In the linear approximation the resonances associated with structural distortions include integer, non-superperiod, and betatron coupling resonances, among which the integer resonances are the strongest.

Due to the small value of the G-factor (gyromagnetic ratio) the resonance map for deuterons is very sparse, and in the momentum range up to 12 GeV/c there are no intrinsic or integer resonances. Therefore the problem of preserving deuteron polarization in the Nuclotron does not exist. The vertical polarization is maintained during the acceleration process and polarized beams can be extracted onto an external target. However obtaining longitudinal polarization of deuterons on an external target using a spin rotator based on transverse magnetic fields is a technically unfeasible task.

In contrast for protons the primary depolarization during acceleration is caused by crossing numerous spin resonances. The number and conditions of these resonances are presented in Table 1, where $\nu = \gamma G$ is the spin tune, $N = 8$ is the number of superperiods of the Nuclotron, and ν_x, ν_y are the betatron oscillation frequencies ($7 < \nu_{x,y} < 7.5$). All frequencies are dimensionless and are understood in units of the particle revolutions.

For decades the Joint Institute for Nuclear Research (JINR) has actively conducted research on depolarizing effects in the Nuclotron and has developed methods to preserve polarization during proton beam acceleration [16–18]. Analysis shows that intrinsic and integer resonances are the primary sources of depolarization in the entire momentum range of the Nuclotron. Coupling and non-superperiod resonances are typically crossed rapidly. The exception are energy regions near intrinsic resonances, where beam depolarization can occur.

For adiabatic crossing of integer resonances article [16] proposed intentionally increasing the resonance strength by introducing a weak longitudinal field. For crossing intrinsic resonances a method was proposed that increases the resonance crossing speed via a betatron frequency jump [19] using fast quadrupoles. This

Table 1. Spin resonances of the linear approximation for protons in the Nuclotron up to 12 GeV/c

Resonance type	Resonance condition	Quantity
Intrinsic	$\nu = kN \pm \nu_y$	4
Integer	$\nu = k$	22
Nonsuperperiodic	$\nu = m \pm \nu_y, (m \neq kN)$	38
Coupling	$\nu = k \pm \nu_x$	43

method was successfully used during the acceleration of polarized particles in the AGS and ZGS synchrotrons [20, 21]. In work [22] it was proposed to perform fast crossing of both intrinsic and integer resonances via a spin frequency jump, which was provided by changing specially established magnetic fields in the Nuclotron.

In methods based on rapid resonance crossing a small beam depolarization always occurs at the level of a few percent, and crossing a large number of resonances ultimately leads to noticeable beam depolarization. A new method of “transparent” crossing, which eliminates beam depolarization, was proposed in [23]. This method was based on matching the spin invariants before and after crossing the resonance region by means of a controlled change in the resonance detuning. However the limiting factors for transparent crossing in the Nuclotron are the spreads in the spin and betatron frequencies.

The possibility of using a partial solenoid snake to preserve polarization during proton acceleration in the Nuclotron was considered in works [24, 25]. A scheme for a partial snake in the energy range up to 6 GeV with compensation of the betatron coupling introduced by the solenoids was proposed in [24]. Abandoning the compensation of betatron coupling made it possible to increase the integral of the longitudinal field for suppressing beam depolarization using a partial solenoid snake [25]. Numerical simulations demonstrated that a 50% snake completely solves the problem of preserving polarization during proton acceleration in the Nuclotron [17].

Dynamic solenoids developed at JINR based on a superconducting NbTi/Cu cable [26] enable the implementation of solenoidal partial snakes in the existing Nuclotron lattice. This paper presents design options for a solenoidal snake in the Nuclotron with and without compensation for betatron coupling. Methods for changing the proton polarization direction are also analyzed, both for an internal target and when extracting the beam from the Nuclotron to an external target.

SOLENOIDAL PARTIAL SNAKES IN THE NUCLOTRON

The “Siberian snake” is a spin rotator that rotates the particle’s spin by 180° around the axis of the snake lying in the accelerator’s plane [27]. There is often insufficient free space to install a snake in already operational accelerators. To suppress spin resonances, it is not necessary to use a “full” snake. It is sufficient to employ a “partial” snake, which requires a smaller integral of the magnetic field, but imposes specific requirements on the choice of betatron frequencies.

When a longitudinal field is introduced into a free interval, the spin frequency becomes a function not only of energy, but also of the spin rotation angle in the solenoid:

$$\cos(\pi\nu) = \cos \frac{\Psi}{2} \cos(\pi\gamma G), \quad \Psi = (1 + G) \frac{(BL)_{\text{sol}}}{B\rho}, \quad (1)$$

where $B\rho$ is the magnetic rigidity. Figure 1 shows the cosine of the spin tune as a function of beam energy for a synchrotron with a partial snake (black line). In the absence of a longitudinal field (red line), $\cos(\pi\nu)$ varies between -1 and $+1$. This inevitably leads to crossings of spin resonances, which are marked by red dots for the series of integer resonances $\nu = k$ and blue dots for the series of intrinsic and non-superperiodic resonances $\nu = k \pm \nu_y$. As the longitudinal field increases, the range of $\cos(\pi\nu)$, equal to $\cos(\Psi/2)$, will decrease. This approach first suppresses the integer spin resonances and subsequently suppresses the intrinsic resonances. In the case of a full snake ($\Psi = \pi$), the graph of $\cos(\pi\nu)$ degenerates into a straight line $\cos(\pi\nu) = 0$, which corresponds to the maximum detuning from integer resonances.

For integer resonances $\gamma G = k$ even a small longitudinal field causes the spin frequency to shift from the resonant value by a magnitude of:

$$|\nu - k| = \frac{\Psi}{2\pi}, \quad (2)$$

and formally the resonance condition $\nu = k$ becomes unattainable. Under real conditions there is a resonance width (resonance strength) that limits the minimum solenoid field value to prevent beam depolarization. The minimum spin tune shift induced by the solenoid must ensure an adiabatic crossing of the spin resonance region. By increasing the integral of the longitudinal field it is also possible to suppress depolarization for a series of resonances with betatron frequencies $\gamma G = k \pm \nu_{x,y}$. This, however, imposes a constraint on the selection of allowable betatron frequency values:

$$\cos(2\pi\nu_{x,y}) > \cos \Psi. \quad (3)$$

During beam acceleration the condition of adiabatic spin motion must be satisfied throughout the entire acceleration cycle. This means that the spin

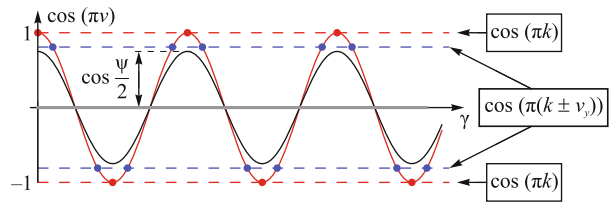


Fig. 1. (Color online) Dependence of $\cos(\pi\nu)$ on beam energy in the Nuclotron with a partial snake.

must complete many revolutions within the characteristic time of the changing solenoid and arc magnet fields. During adiabatic acceleration the spin will follow the precession axis, which will change its components during the acceleration process. For a partial snake the precession axis \mathbf{n} in the opposite straight section lies in the vertical plane (yz):

$$\mathbf{n} = \frac{\sin \frac{\Psi}{2} \mathbf{e}_z + \cos \frac{\Psi}{2} \sin(\pi\gamma G) \mathbf{e}_y}{\sqrt{1 - \cos^2 \frac{\Psi}{2} \cos^2(\pi\gamma G)}}. \quad (4)$$

Here, \mathbf{e}_y , \mathbf{e}_z are the vertical and longitudinal unit vectors of the accelerator coordinate system respectively. The \mathbf{n} -axis deviates significantly from the vertical, periodically aligning with the velocity at energy values corresponding to $\gamma G = k$. In this case the spin dynamics become analogous to the case of a 100% snake, where $\Psi = \pi$. Due to the spread in the spin tune the beam polarization is directed along the \mathbf{n} -axis.

Figure 2 shows the layout of the partial snake in the Nuclotron along with the beam injection/extraction

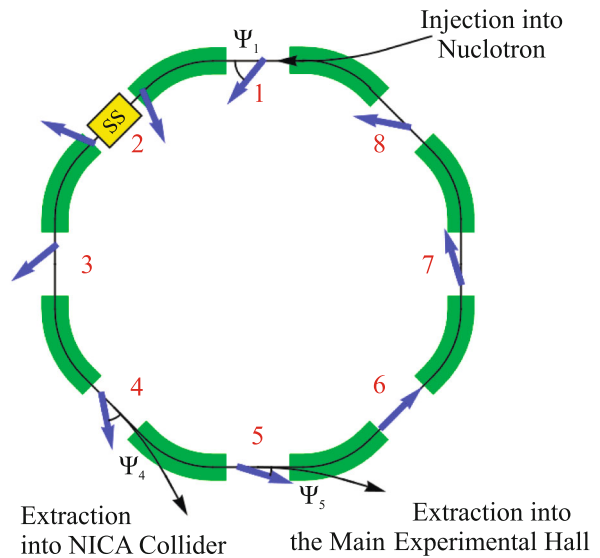


Fig. 2. (Color online) Location of the solenoidal partial snake in the Nuclotron.

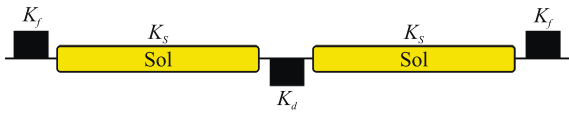


Fig. 3. (Color online) Layout of the partial snake employing betatron coupling.

points: the snake is located in the second straight section, beam injection from the LU-20 linear accelerator is performed in the first section, and beam extraction from the Nuclotron to the NICA collider and to the experimental hall is performed in the fourth and fifth sections respectively. Also, in Fig. 2, the dynamics of the \mathbf{n} -axis along the Nuclotron ring for the case of a 100% snake are shown with blue arrows. In the opposite (sixth) straight section, the polarization is directed along the beam velocity. As the beam moves towards the snake, the polarization is rotated by the arc dipoles through an angle $\pi\gamma G$. Subsequently the snake rotates the polarization around the longitudinal direction by 180° (reflecting it relative to the direction of velocity in the ring plane), and it returns to its original longitudinal direction as it approaches the sixth straight section. For a partial snake the dynamics of the transverse polarization components will be similar to the case of a full snake, and in addition a constant vertical spin component will appear in the Nuclotron outside the snake.

Figure 3 shows a schematic of the partial snake without betatron coupling suppression, which efficiently utilizes the available space in the second superperiod of the Nuclotron. At a maximum solenoid field of 5 T and a single solenoid length of 2.8 m, the total longitudinal field integral is 28 T m (approximately a 60% snake). In the strong-focusing FODO lattice of the Nuclotron the vertical and radial betatron oscillation frequencies are close to each other. In the presented layout as the snake strength increases, the main contribution to beam depolarization will come from the coupling resonances excited by the solenoids, which are located near the intrinsic resonances.

Figure 4 presents the results of simulating proton acceleration in the Nuclotron with a 60% snake and betatron coupling, performed using the Zgoubi spin-tracking code [28]. The calculations assumed betatron frequencies of $\nu_x = 6.9$ and $\nu_y = 7.15$, a normalized emittance of 2.0 mm mrad, and the initial spin orientation along the \mathbf{n} -axis. Proton acceleration was limited to the critical energy, approximately equal to 11 GeV. Spin observation was conducted in the straight section of the sixth superperiod of the Nuclotron, opposite the snake. The top part of Fig. 4 shows the dynamics of the spin projections S_x, S_y, S_z onto the unit vectors of the accelerator coordinate system, which fully agrees with formula (5). The bottom part shows the projection of the spin onto the \mathbf{n} -axis (S_n),

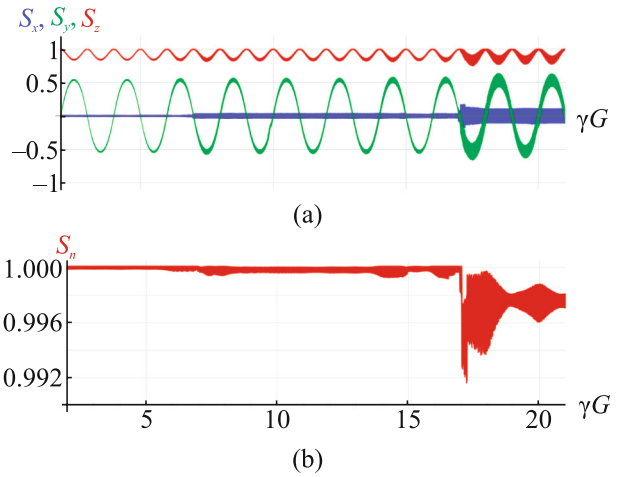


Fig. 4. (Color online) Proton spin dynamics during acceleration in the presence of a partial snake and without coupling compensation: (a) evolution of the spin components (b) projection of the spin vector onto the \mathbf{n} -axis.

which remains practically unchanged during the acceleration process. A minor change in the S_n projection, not exceeding 0.5%, occurs in energy regions corresponding to coupling resonances.

A schematic of the partial snake with suppressed betatron coupling, utilizing four solenoids, is shown in Fig. 5. Coupling compensation was achieved with four quadrupoles rotated by $\pm 45^\circ$. The total longitudinal field integral with a single solenoid length of 1.2 m is 24 T m (approximately a 50% snake). In this layout due to the localization of the betatron coupling within the solenoid section, the strength of the coupling resonances will be significantly lower than in the scheme with coupling.

Figure 6 presents a similar result from simulating proton acceleration in the Nuclotron with a 50% snake and compensated betatron oscillation coupling. The calculations assumed betatron frequencies of $\nu_x = 7.12$ and $\nu_y = 7.12$, a normalized emittance of 2.0 mm mrad, and the spin initially oriented along the \mathbf{n} -axis. The simulation results are in complete agreement with theoretical calculations. As expected, due to the localization of the coupling in the snake section the deviation of the spin projection on the \mathbf{n} -axis remains practically unchanged throughout the entire acceleration range.

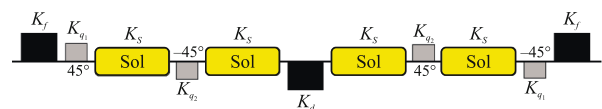


Fig. 5. (Color online) Layout of the partial snake with betatron coupling suppression.

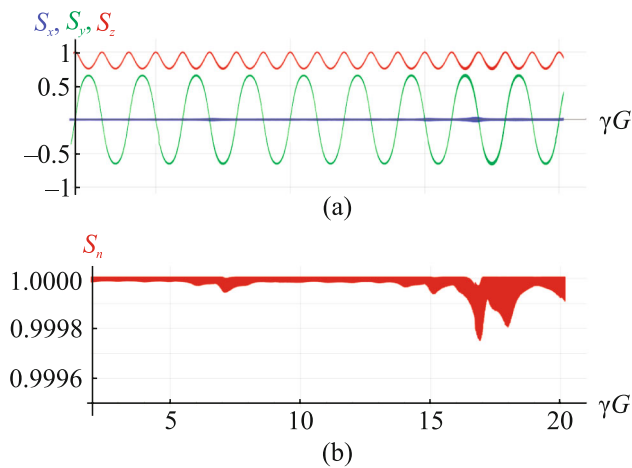


Fig. 6. (Color online) Proton spin dynamics during acceleration in the presence of a partial snake and with coupling compensation: (a) evolution of the spin components (b) projection of the spin vector onto the \mathbf{n} -axis.

Currently a solenoid made from HTSP tape has been manufactured and tested at JINR in helium vapor and liquid nitrogen. It achieves a central field of up to 5.6 T and a field ramp rate of about 1 T/s. Such solenoids can be used in the proposed layouts of partial snakes both with and without compensation of betatron oscillation coupling. The ability to change the solenoid field proportionally to the beam momentum makes it possible to stabilize the frequencies and optical characteristics of betatron oscillations during the proton acceleration process.

POLARIZATION MATCHING DURING INJECTION INTO THE NUCLOTRON

To preserve the degree of polarization it is necessary to ensure collinearity between the \mathbf{n} -axis and the spins of the injected particles at the injection point. When operating with partial snakes, the direction of the \mathbf{n} -axis in the first straight section of the Nuclotron, where proton injection occurs, is determined by the spin rotation angle in the snake Ψ (see Fig. 7). For a full snake the $\Psi = \pi$ \mathbf{n} -axis lies in the plane of the Nuclotron, while with the snake turned off, the \mathbf{n} -axis is directed vertically.

This matching can be achieved in several ways. For example, two solenoids can be installed in the transport channel from the LU-20 linear accelerator to the Nuclotron [29]. These solenoids will allow to alter the spin direction of the injected beam to the required direction of the \mathbf{n} -axis at the injection point. In this case when the polarization is matched during beam injection, the structural functions of the synchrotron will remain unchanged.

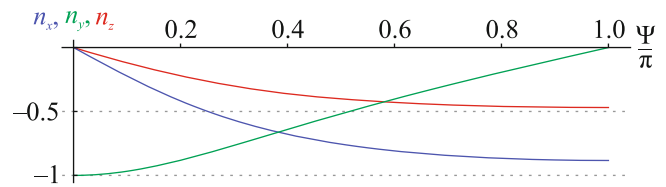


Fig. 7. (Color online) Components of the \mathbf{n} -axis in the first straight section of the Nuclotron.

Another possibility is to install two solenoids directly in the Nuclotron and perform the matching by adjusting the \mathbf{n} -axis to the specified polarization direction of the beam at the injection point. The first option is to use snake solenoid for this task. The second solenoid must be placed in another straight section. With this approach after matching the solenoids must be adjusted adiabatically: the second solenoid is turned off, and the snake solenoids are switched to their operational mode at the injection plateau. The required field integrals of the solenoids for polarization matching will be approximately ~ 0.4 T m.

POLARIZATION CONTROL DURING BEAM EXTRACTION TO THE TARGET

The presented snake layouts solve the problem of preserving proton polarization within the momentum range of the Nuclotron. Furthermore for experiments with extracted beams it is necessary to solve the problem of the spin direction control at the external target. The direction of the proton polarization in the fifth straight section, from which the beam is extracted from the Nuclotron to the experimental hall, will be a function of energy. For demonstration Fig. 8 shows the components of the \mathbf{n} -axis during the extraction of the proton beam from the Nuclotron for a 60% snake.

The required polarization direction of protons at the external target can be provided by a spin rotator installed in the beam transport channel to the experimental hall. For example, a solenoid with a field integral of up to ± 22 T m can be used to rotate the polarization into the vertical plane of the target over the entire momentum range. Subsequently, longitudinal or vertical polarization can be obtained using a radial rotator with a fixed orbit, whose layout is shown in

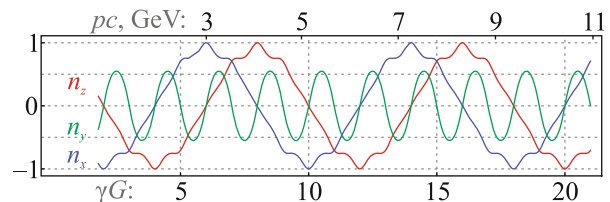


Fig. 8. (Color online) Components of the \mathbf{n} -axis during beam extraction from the Nuclotron.

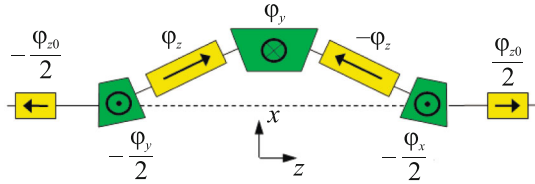


Fig. 9. (Color online) Layout of the radial rotator with a fixed orbit bump.

Fig. 9. A rotator of this type, rotating spins by small angles, was used for polarization stabilization in the radial direction in the MEIC project (Jefferson Lab) [30, 31].

To fix the beam orbit in the rotator, the dipole fields must be changed proportionally to the beam momentum. The solenoid field values are chosen according to the relations:

$$\sin \frac{\phi}{4} = \sin \frac{\varphi_y}{4} \sin \frac{\varphi_z}{4}, \quad \tan \frac{\varphi_{z0}}{4} = \cos \frac{\varphi_y}{4} \tan \frac{\varphi_z}{4}, \quad (5)$$

controlled rotation of the spin around the radial direction by an angle ϕ can be achieved. Here, φ_y , φ_z , φ_{z0} are the spin rotation angles in the dipole magnets and solenoids respectively. To achieve any proton polarization direction in the vertical plane ($|\phi| \leq \frac{\pi}{2}$) at the external target within the momentum range from 2 to 12 GeV/c, the required integrals of the longitudinal and vertical fields are approximately equal to 35 and 15 T m, respectively.

The control of proton polarization at the external target can also be achieved without the aforementioned spin rotators. Longitudinal or transverse polarization can be provided using weak magnetic fields (spin navigators) directly in the Nuclotron at discrete energies corresponding to integer spin resonances, which occur in steps of 523 MeV. Spin navigators based on two weak solenoids for the Nuclotron were proposed in [32]. Spin navigators based on steer dipoles, which allow for the control of proton polarization via controlled distortion of the Nuclotron's closed orbit, were proposed in [33].

CONCLUSIONS

The proposed partial snakes with and without betatron oscillation coupling compensation make it possible, in principle, to suppress the resonant depolarization of the beam during proton acceleration over the entire momentum range of the Nuclotron. With proper matching of the polarization direction during beam injection into the Nuclotron the polarization degree at the output of the Nuclotron can in the limit reach for 80% obtained at the output of the polarized proton source [7]. To form high-intensity polarized proton beams for the NICA collider [34] with an aver-

age luminosity of up to $10^{32} \text{ cm}^{-2} \text{ s}^{-1}$ the LILAC linear accelerator [35] is planned for particle injection into the Nuclotron. In this case the characteristic number of accelerated polarized protons at the output of the Nuclotron can reach up to 5×10^{10} particles per cycle. The proposed partial snake configurations are relevant both for the existing Nuclotron lattice and for a potentially new magnetic-optical lattice if the Nuclotron is upgraded to increase the luminosity of the NICA collider when operating with polarized beams.

An additional weak solenoid makes it possible to control the polarization direction at discrete energies corresponding to integer spin resonances both inside the Nuclotron and at external targets. It will become possible to use the Nuclotron for experimental verification of the spin transparency concept, as well as a test bench for debugging polarization control and measurement systems in the ST (Spin Transparency) mode.

The proposed spin rotator with a fixed orbit in the beam transport line will allow for obtaining any spin orientation in the vertical plane at the external target over the entire energy range. The delivery of beams with any controlled polarization to the external target is important for new approaches to searching for milli-strong CP-violation beyond the Standard Model via vector-tensor asymmetry and for observing P-odd asymmetry in the total scattering cross section of polarized protons and deuterons. Beyond the proposed precision tests of the standard electroweak theory, which measure P-odd asymmetry using oscillating horizontal polarization [36, 37], experiments with stationary longitudinal polarization will become feasible. This alternative approach will be enabled by the use of spin navigators in the ST mode and spin rotators in the transport channel.

It is becoming feasible to conduct experiments in the NICA collider in the spin transparency mode without using solenoid snakes by injecting polarized protons from the Nuclotron at energies corresponding to integer spin resonances [38]. In this case the question of beam cooling at proton collision energies to achieve the required luminosity remains open.

An opportunity is opening up to conduct experiments with polarized protons both on external and internal targets in the Nuclotron, independently or in parallel with the execution of experiments in the heavy-ion mode of the NICA collider. Experiments with polarized beams in the Nuclotron will significantly expand the program of fundamental research in the physics of particle spins at the NICA facility.

FUNDING

This work was supported by the ongoing funding of the Moscow Institute of Physics and Technology (National Research University) and the Joint Institute for Nuclear

Research. No additional grants to carry out or direct this particular research were obtained.

CONFLICT OF INTEREST

The authors of this work declare that they have no conflicts of interest.

OPEN ACCESS

This article is licensed under a Creative Commons Attribution 4.0 International License, which permits use, sharing, adaptation, distribution and reproduction in any medium or format, as long as you give appropriate credit to the original author(s) and the source, provide a link to the Creative Commons license, and indicate if changes were made. The images or other third party material in this article are included in the article's Creative Commons license, unless indicated otherwise in a credit line to the material. If material is not included in the article's Creative Commons license and your intended use is not permitted by statutory regulation or exceeds the permitted use, you will need to obtain permission directly from the copyright holder. To view a copy of this license, visit <http://creativecommons.org/licenses/by/4.0/>

REFERENCES

1. V. D. Kekelidze, A. D. Kovalenko, I. N. Meshkov, A. S. Sorin, and G. V. Trubnikov, *Phys. At. Nucl.* **75**, 542 (2012).
2. K. Abraamyan, S. Afanasiev, V. Alfeev, et al., *Nucl. Instrum. Methods Phys. Res., Sect. A* **628**, 99 (2011).
3. V. Abazov, V. Abramov, L. Afanasyev, et al., *Nat. Sci. Rev.* **1**, 1 (2024).
4. I. Savin, A. Efremov, D. Peshekhonov, A. Kovalenko, O. Teryaev, O. Shevchenko, A. Nagajcev, A. Guskov, V. Kukhtin, and N. Topilin, *EPJ Web of Conf.* **85**, 02039 (2015).
5. V. Abramov, A. Aleshko, V. Baskov, E. Boos, V. Bunichev, O. Dalkarov, R. El-Kholy, A. Galoyan, A. Guskov, and V. Kim, *Phys. Part. Nucl.* **52**, 1044 (2021).
6. A. Baldin, S. Averichev, Y. Beznogikh, et al., *IEEE Trans. Nucl. Sci.* **30**, 3247 (1983).
7. V. Fimushkin, A. D. Kovalenko, L. V. Kutuzova, Y. V. Prokofichev, V. B. Shutov, A. S. Belov, V. N. Zubits, and A. V. Turbabin, in *Proceedings of the 16th International Workshop in Polarized Sources, Targets, and Polarimetry*, PoS (PSTP2015) (2016).
8. P. Kurilkin, V. Ladygin, T. Uesaka, et al., *Nucl. Instrum. Methods Phys. Res., Sect. A* **642** (1), 45 (2011).
9. A. A. Terekhin, I. S. Volkov, Y. V. Gurchin, A. Y. Isupov, V. P. Ladygin, S. G. Reznikov, A. V. Tishevsky, A. N. Khrenov, and M. Janek, *Phys. Part. Nucl.* **54**, 634 (2023).
10. L. Azhgirey, V. Ladygin, F. Lehar, A. Prokofiev, G. Stoletov, A. Zhdanov, and V. Zhmyrov, *Nucl. Instrum. Methods Phys. Res., Sect. A* **497**, 340 (2003).
11. V. P. Ladygin, A. V. Averyanov, E. V. Chernykh, et al., *JPS Conf. Proc.* **37**, 020902 (2022).
12. A. A. Druzhinin, N. M. Piskunov, R. A. Shindin, Y. T. Kiryushin, D. A. Kirillov, N. V. Kostiaeva, E. P. Makoveev, and A. E. Baskakov, *Phys. Part. Nucl.* **55**, 1086 (2024).
13. S. N. Basilev, Y. P. Bushuev, O. P. Gavrishchuk, et al., *Eur. Phys. J. A* **56**, 26 (2020).
14. V. Ladygin, *PoS (BaldinISHEPPXXII)*, 098 (2014).
15. S. Vokal, A. D. Kovalenko, A. M. Kondratenko, M. A. Kondratenko, V. A. Mikhailov, Y. N. Filatov, and S. S. Shimanskii, *Phys. Part. Nucl. Lett.* **6**, 48 (2009).
16. N. Golubeva, I. Issinskij, V. Mikhajlov, E. Stokovskij, A. Kondratenko, and M. Kondratenko, Preprint JINR P9-2002-289 (Joint Inst. Nucl. Res., Dubna, 2002).
17. Y. Filatov, A. Butenko, A. Kondratenko, M. Kondratenko, A. Kovalenko, and V. Mikhaylov, in *Proceedings of the International Particle Accelerator Conference IPAC'17* (2017), Vol. 8, p. 2349.
18. Y. N. Filatov, A. M. Kondratenko, M. A. Kondratenko, S. V. Vinogradov, E. D. Tsyplakov, A. V. Butenko, S. A. Kostromin, V. P. Ladygin, E. M. Syresin, and E. A. Butenko, *Phys. Part. Nucl.* **55**, 731 (2024).
19. Y. M. Shatunov, I. A. Koop, A. V. Otboev, S. P. Mane, and P. Y. Shatunov, *Phys. Part. Nucl. Lett.* **15**, 315 (2018).
20. L. Ratner, H. Brown, I. Chiang, et al., *IEEE Trans. Nucl. Sci.* **32**, 1656 (1985).
21. L. G. Ratner and T. K. Khoe, *IEEE Trans. Nucl. Sci.* **20**, 217 (1973).
22. N. Golubeva, A. Kondratenko, and Y. Filatov, in *Proceedings of the International Workshop Deuteron-93* (1994), p. 374.
23. A. Kondratenko, M. Kondratenko, and Y. Filatov, *Phys. Part. Nucl. Lett.* **1**, 266 (2004).
24. Y. N. Filatov, A. D. Kovalenko, A. V. Butenko, A. M. Kondratenko, M. A. Kondratenko, and V. A. Mikhaylov, *Phys. Part. Nucl.* **45**, 262 (2014).
25. Y. N. Filatov, A. V. Butenko, A. M. Kondratenko, M. A. Kondratenko, A. D. Kovalenko, and V. A. Mikhaylov, in *Proceedings of the International Particle Accelerator Conference IPAC'14* (2014), p. 1162.
26. H. G. Khodzhbagiyani, P. G. Akishin, A. V. Butenko, A. V. Bychkov, G. L. Kuznetsov, M. S. Novikov, E. V. Sergeeva, G. V. Trubnikov, E. S. Fischer, and A. V. Shemchuk, *Nat. Sci. Rev.* **1**, 6 (2024).
27. Y. Derbenev, Y. Filatov, A. Kondratenko, M. Kondratenko, and V. Morozov, *Symmetry* **13**, 398 (2021).
28. F. Méot, *Nucl. Instrum. Methods Phys. Res., Sect. A* **427**, 353 (1999).
29. A. Kovalenko, A. Butenko, V. Mikhaylov, M. Kondratenko, A. Kondratenko, and Y. Filatov, *J. Phys.: Conf. Ser.* **938**, 012018 (2017).
30. Y. Derbenev, F. Lin, V. Morozov, Y. Zhang, A. Kondratenko, and M. Kondratenko, in *Proceedings of the International Particle Accelerator Conference IPAC'15* (2015), p. 2301.
31. Y. N. Filatov, A. M. Kondratenko, M. A. Kondratenko, Y. S. Derbenev, V. S. Morozov, A. V. Butenko, E. M. Syresin, and E. D. Tsyplakov, *Eur. Phys. J. C* **81**, 986 (2021).

32. Y. Filatov, A. Kondratenko, M. Kondratenko, V. Vorobyov, S. Vinogradov, E. Tsyplakov, A. Butenko, E. Syresin, S. Kostromin, Y. Derbenev, and V. Morozov, *J. Instrum.* **16**, P12039 (2021).
33. Y. Filatov, A. Kondratenko, N. Nikolaev, Y. Senichev, M. Kondratenko, S. Vinogradov, E. Tsyplakov, A. Butenko, S. Kostromin, V. Ladygin, E. Syresin, I. Guryleva, A. Melnikov, and A. Aksentyev, *JETP Lett.* **118**, 387 (2023).
34. E. Syresin, A. Butenko, P. Zenkevich, O. Kozlov, S. Kolokolchikov, S. Kostromin, I. Meshkov, N. Mityanina, Y. Senichev, A. Sidorin, and G. Trubnikov, *Phys. Part. Nucl.* **52**, 997 (2021).
35. B. Koubek et al., in *Proceedings of the 29th Linear Accelerator Conference LINAC'18* (2019), Vol. 29, p. 362.
36. I. A. Koop, A. I. Milstein, N. N. Nikolaev, A. S. Popov, S. G. Salnikov, P. Y. Shatunov, and Y. M. Shatunov, *Phys. Part. Nucl. Lett.* **17**, 154 (2020).
37. I. A. Koop, A. I. Milstein, N. N. Nikolaev, A. S. Popov, S. G. Salnikov, P. Y. Shatunov, and Y. M. Shatunov, *Phys. Part. Nucl.* **52**, 549 (2021).
38. Y. Filatov, A. Kovalenko, A. Butenko, E. Syresin, V. Mikhailov, S. Shimanskiy, A. Kondratenko, and M. Kondratenko, *Eur. Phys. J. Web Conf.* **204**, 10014 (2019).

Translated by the authors

Publisher's Note. Pleiades Publishing remains neutral with regard to jurisdictional claims in published maps and institutional affiliations. AI tools may have been used in the translation or editing of this article.